

Highly efficient four-wave parametric amplification in transparent bulk Kerr medium

A. Dubietis¹, G. Tamošauskas¹, P. Polesana^{1*}, G. Valiulis¹,
H. Valtna^{1**}, D. Faccio², P. Di Trapani^{1*}, A. Piskarskas¹

¹*Department of Quantum Electronics, Vilnius University, Saulėtekio Ave. 9, bldg.3, LT-10222 Vilnius, Lithuania*

²*Dipartimento di Fisica Università dell'Insubria, via Vallegio 11, IT-22100 Como, Italy*
audrius.dubietis@ff.vu.lt

Abstract: We report on highly efficient four-wave optical parametric amplification in a water cell pumped by an elliptically shaped, ultrashort pulsed laser beam under non-collinear phase-matching configuration. Energy conversion from pump to parametric waves as high as 25 % is obtained owing to the achievement of 1-dimensional spatial-soliton regime, which guarantees high intensity over a large interaction length and ensures high beam quality.

© 2007 Optical Society of America

OCIS codes: (190.4380) Nonlinear optics, four-wave mixing; (190.5530) Pulse propagation and solitons

References and links

1. M. H. Dunn and M. Ebrahimzadeh, "Parametric generation of tunable light from continuous-wave to femtosecond pulses," *Science* **286**, 1513–1517 (1999).
2. G. Cerullo and S. De Silvestri, "Ultrafast optical parametric amplifiers," *Rev. Sci. Instrum.* **74**, 1–18 (2003).
3. A. Dubietis, R. Butkus, and A. Piskarskas, "Trends in chirped pulse optical parametric amplification," *IEEE J. Sel. Top. Quantum Electron.* **12**, 163–172 (2006).
4. G. P. Agrawal, *Nonlinear Fiber Optics*, Academic Press, San Diego, CA, 1989.
5. K. Inoue and T. Mukai, "Signal wavelength dependence of gain saturation in a fiber optical parametric amplifier," *Opt. Lett.* **26**, 10–12 (2001).
6. M. E. Marhic, K. K. Y. Wong, M. C. Ho, and L. G. Kazovsky, "92% pump depletion in a continuous-wave one-pump fiber optical parametric amplifier," *Opt. Lett.* **26**, 620–622 (2001).
7. R. R. Alfano and S. L. Shapiro, "Emission in the region 4000 to 7000 Å via four-photon coupling in glass," *Phys. Rev. Lett.* **24**, 584–587 (1970).
8. A. Penzkofer, A. Laubereau, and W. Kaiser, "Stimulated short-wave radiation due to single-frequency resonances of $\chi^{(3)}$," *Phys. Rev. Lett.* **31**, 863–866 (1973).
9. A. Penzkofer and H. J. Lehmeier, "Theoretical investigation of noncollinear phase-matched parametric four-photon amplification of ultrashort light pulses in isotropic media," *Opt. Quantum Electron.* **25**, 815–844 (1993).
10. H. Crespo, J. T. Mendonça, and A. Dos Santos, "Cascaded highly nondegenerate four-wave-mixing phenomenon in transparent isotropic condensed media," *Opt. Lett.* **25**, 829–831 (2000).
11. F. Théberge, N. Aközbek, W. Liu, A. Becker, and S. L. Chin, "Tunable ultrashort laser pulses generated through filamentation in gases," *Phys. Rev. Lett.* **97**, 023904 (2006).
12. H. Schroeder, J. Liu, and S. L. Chin, "From random to controlled small-scale filamentation in water," *Opt. Express* **12**, 4768–4774 (2004), <http://www.opticsinfobase.org/abstract.cfm?URI=oe-12-20-4768>.
13. M. Centurion, Y. Pu, and D. Psaltis, "Self-organization of spatial solitons," *Opt. Express* **13**, 6202–6211 (2005), <http://www.opticsinfobase.org/abstract.cfm?URI=oe-13-16-6202>.
14. A. Dubietis, E. Kučinskas, and G. Tamošauskas, "Formation of periodic multifilamentary structures by use of highly elliptical light beams," *Lithuanian J. Phys.* **47**, 27–30 (2007).
15. A. Barthelemy, S. Maneuf, and C. Froehly, "Propagation soliton et auto-confinement de faisceaux laser par non linéarité optique de Kerr," *Opt. Commun.* **55**, 201–206 (1985).

16. M. Soljačić, S. Sears, and M. Segev, "Self-trapping of "Necklace" beams in self-focusing Kerr media," *Phys. Rev. Lett.* **81**, 4851–4854 (1998).
 17. C. Anastassiou, M. Soljačić, M. Segev, E. D. Eugenieva, D. N. Cristodoulides, D. Kip, Z. H. Musslimani, and J. P. Torres, "Eliminating the transverse instabilities of Kerr solitons," *Phys. Rev. Lett.* **85**, 4888–4891 (2000).
 18. P. B. Lundquist, D. R. Andersen, and Y. S. Kivshar, "Multicolor solitons due to four-wave mixing," *Phys. Rev. E* **57**, 3551–3555 (1998).
 19. G. Fanjoux, J. Michaud, M. Delqué, H. Mailotte, and T. Sylvestre, "Generation of multicolor Kerr solitons by cross-phase modulation, four-wave mixing, and stimulated Raman scattering," *Opt. Lett.* **31**, 3480–3482 (2006).
 20. A. G. Van Engen, S. A. Diddams, and T. S. Clement, "Dispersion measurements of water with white-light interferometry," *Appl. Opt.* **37**, 5679–5686 (1998).
 21. R. M. Pope and E. S. Fry, "Absorption spectrum (380-700 nm) of pure water. II. Integrating cavity measurements," *Appl. Opt.* **36**, 8710–8723 (1997).
-

1. Introduction

Optical parametric amplification *via* three-wave interaction in non centrosymmetric materials is nowadays a well established technique, used for producing powerful ultrashort light pulses tunable across wide spectral range [1, 2, 3]. For the case of non-resonant isotropic media, the lowest-order supported interaction is the four-wave mixing (FWM) driven by the third-order susceptibility, which is much less efficient owing to smaller nonlinear response. Up to date, most of the investigations concerning Kerr-driven FWM parametric processes have been conducted in the framework of fiber optics [4], demonstrating high energy conversion efficiency in ns-pulse and continuous wave regime at telecom wavelengths [5, 6]. In the ultrashort pulse regime, studies in the past were directed to generation of broadband parametric radiation (white-light continuum) in transparent bulk Kerr media under different operating regimes [7, 8], for spectroscopy applications. Theoretical foundations for ultrashort pulse four-wave parametric amplification in transparent bulk media had been put forward by Penzkofer and Lehmeier in their detailed review paper [9], outlining competing processes such as stimulated Raman scattering, self-focusing, self- and cross-phase modulation and optical breakdown as major difficulties to achieve efficient performance under real experimental settings. Experimentally, non-collinear phase-matched frequency mixing of two intense femtosecond pulses has been demonstrated in a thin BK7 glass plate [10]. However, due to onset of material damage under the chosen tightly focusing configuration, the generated pulse energy was limited to few μJ only. A different approach that exploits a long interaction path has been proposed by Théberge and coauthors, who have obtained four-wave parametric amplification in a single gas filament [11]. The results outlined high beam quality but low (*i.e.* $\simeq 10^{-3}$) energy conversion from the pump to the generated waves despite large pump energy (1 mJ), since the collinear interaction geometry does not take an advantage of linear phase-matching. Moreover, the proposed approach is not re-scalable in energy, the beam width being locked to the filament dimension.

In this Paper we report on highly efficient performance of seeded, water-based four-wave optical parametric amplifier (FWOPA), which utilizes noncollinear phase-matched interaction in elliptical beam geometry. An excellent FWOPA operation is obtained by achieving FWM-mediated 1-dimensional optical spatial solitary waves in bulk water sample, which ensure high beam quality and high parametric gain over long interaction length.

2. Results and discussion

The experiment was performed using a Nd:glass laser system (Twinkle, Light Conversion Ltd., Lithuania) delivering frequency-doubled 1-ps, 4-mJ pulses at 527 nm at 10 Hz repetition rate. The laser output was split into two parts. The first portion of the laser radiation was spatially filtered and made variable in energy (by a combination of a $\lambda/2$ -plate and thin-film polarizer) and then utilized as a pump for the FWOPA. The second portion pumped a frequency-doubled

optical parametric generator (Topas, Light Conversion Ltd., Lithuania), which delivered 0.5-ps pulses tunable across the visible. After spatial filtering and suitable attenuation, selected "signal" pulses at $\lambda_s = 570$ nm or $\lambda_s = 490$ nm were used to seed the FWOPA. Both, pump and signal pulses were adjusted in time by means of an optical delay line and focused into 40-mm-long water cell using a cylindrical lens of $f_x = +500$, $f_y = \infty$, yielding beam dimensions of 1.2 mm \times 130 μ m at the input face of the cell, as shown in Fig. 1(a). The angle between pump and signal beams was adjusted for largest energy conversion due to optimum phase matching. The two beams were crossed in the plane containing the long axes of the ellipses in order to optimize spatial overlap across the beam path along the entire sample.

It is known that highly elliptical beams with power much exceeding the critical power for self-focusing break-up into arrays of multiple filaments [12, 13]. In our settings, pump beam with $E_p > 50$ μ J experiences 1-dimensional self-focusing in the short-axis direction and after passing the nonlinear focus eventually breaks-up into an array of almost equally spaced multiple filaments [14], as depicted in Fig. 1(b). Filamentation is accompanied by conical emission, producing a complex interference pattern in the far-field, shown in Fig. 1(d). By contrast, the injection of the weak seed at the phase matching angle leads to the quenching of beam break-up, as apparent in Fig. 1(c), so that no filaments were formed for E_p as large as 80 μ J. Concomitantly, four-wave parametric amplification of the seed pulse is accompanied by the emergence of a comb of discrete up and down-shifted frequencies that result from high order cascaded FWM process, as evident from the far-field pattern in Fig. 1(e). The seeding, however, does not inhibit 1-dimensional self focusing. As a consequence, an intense and spatially clean pump beam profile develops and propagates for a fairly long distance inside the sample, optimally overlapped with the non-collinear seed, thus providing an ideal condition for efficient parametric FWM process to take place.

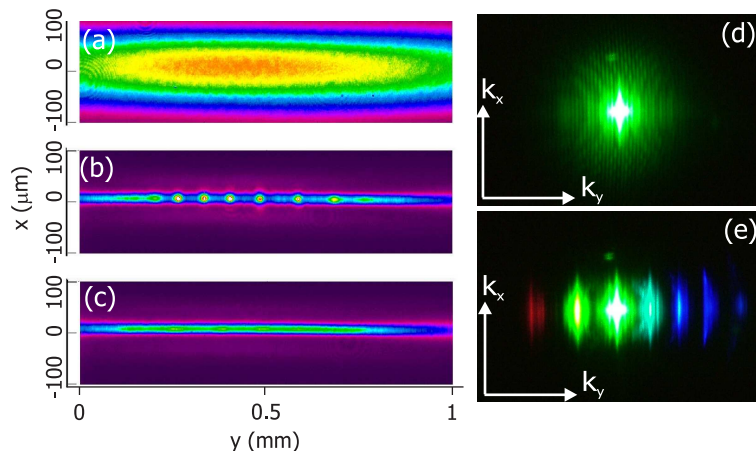


Fig. 1. Near field intensity profiles of the pump beam at the 40-mm-long water cell input (a) and output: (b) without and (c) with the seed signal. Screen shots representing the far-field: (d) without and (e) with seed signal. Pump pulse energy is 75 μ J.

A closer inspection of the pump beam propagation inside the sample revealed the achievement of 1-dimensional spatial soliton regime, *i.e.* the beam that preserves its shape and dimension in one transverse coordinate during propagation. Fig. 2 shows the dependence of FWHM pump-beam short-axis diameter on propagation length, as obtained by monitoring the output beam profile for fixed input energy condition ($E_p = 75$ μ J) and different lengths of the cuvette. The overall observation implies a diffraction-free propagation of 24 μ m FWHM diame-

ter beam, which starts at ≈ 25 mm from the input face of the cuvette, over a distance of ≈ 15 mm that is 4.5 times larger than the linear diffraction length, $z_R = 3.3$ mm for a Gaussian beam of the same diameter. Moreover, the signal and idler modes exhibit a high beam quality and diffraction-free propagation inside the nonlinear medium as well being trapped within the intense gain channel provided by the pump beam. Up to date, stable spatial solitons in bulk Kerr media were observed just on several occasions, where transverse instabilities were suppressed by self-induced-waveguiding through interference [15], periodic azimuthal modulation of ring beams [16] and by the use of partially incoherent light beams [17]. The present situation differs also from the multicolor parametric soliton regime in planar waveguides, since they are known [18] and recently experimentally demonstrated [19] to support 1-dimensional spatial solitons under strong FWM interaction. Clarifying the mechanism that leads to instability quenching in bulk Kerr medium is out of the purpose of this work, here we just mention that an increase in the pump beam breakup threshold has to be reasonably expected in presence of non-collinear interaction, off-axis (signal and idler) modes acting as a damping mechanism that drains power away from any local spike that eventually forms in the pump beam.

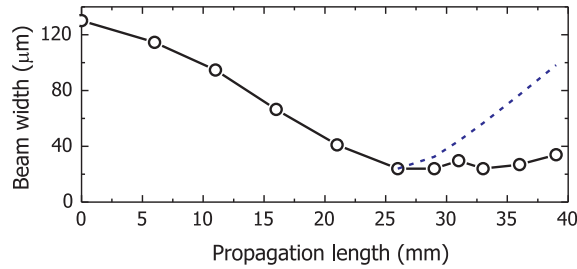


Fig. 2. Open circles: measured pump beam FWHM diameter vs propagation distance. Dashed line: calculated diffraction spreading of 24 μm Gaussian beam.

Figure 3(a) illustrates the measured output-pulse energy for the signal and the corresponding idler pulses vs the input pump energy, for the case of seeding by ≈ 0.1 μJ pulses at $\lambda_s = 570$ nm. The result outlines a signal amplification factor of 100, with 15% pump-to-signal energy conversion at $E_p = 60$ μJ , where gain saturation occurs. At saturation the overall energy conversion to parametric waves as high as 25 % is measured. Surprisingly, a sizable energy unbalance is detected, the idler wave remaining $\simeq 3.5$ times weaker than the signal in the entire saturation regime. Interestingly, virtually the same unbalance holds when the role of the signal and idler waves is inverted, *i.e.* when the FWOPA is seeded at $\lambda_s = 490$ nm, as evident from the results shown in Fig. 3(b).

In order to ascertain the mechanism that leads to the apparent unbalance in measured signal and idler wave energy, we examine in detail the phase-matching, energy and photon-number distribution over the entire set of cascaded waves. Figure 4(a) (circles) shows the measured angles and corresponding wavelengths for 3 red-shifted and 5 blue-shifted side bands, for operating conditions reported in Fig. 3(a). The solid line represents the computed non-collinear phase matching curve for the (linear) FWM process $\mathbf{k}_p + \mathbf{k}_p = \mathbf{k}_s + \mathbf{k}_i$, where $k(\omega) = n(\omega)\omega/c$ is the wave number obeying the dispersion relation for water [20] and indexes p, s, i stand for the pump, signal and idler waves, respectively. The cascaded modes are generated through the multi-step FWM processes [10]: $\mathbf{k}_{s1} = 2\mathbf{k}_s - \mathbf{k}_p$, $\mathbf{k}_{i1} = 2\mathbf{k}_i - \mathbf{k}_p$, $\mathbf{k}_{i2} = 2\mathbf{k}_{i1} - \mathbf{k}_i$, etc., where numerical indexes denote the cascading order. Note that, for the chosen signal injection angle $\theta_s = 0.75^\circ$ (in water), the deviation from exact phase matching remains minimal for the first 3-4 cascaded modes, which entails efficient cascading over a quite broad spectral range. Figure 4(b) reports the energy contents of the closest sidebands, for seeding at $\lambda_s = 570$ nm and pumping

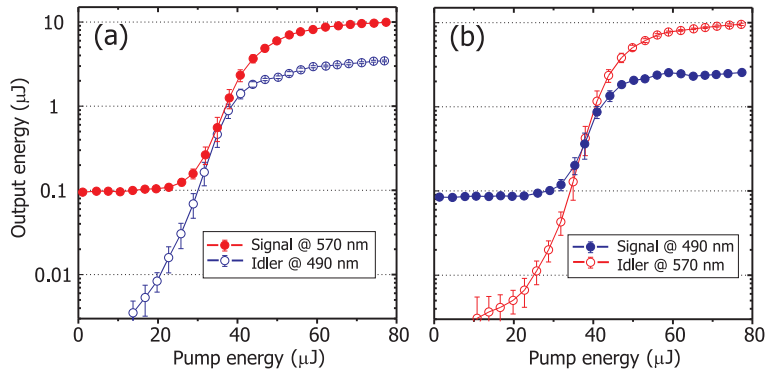


Fig. 3. Operational characteristics of the FWOPA seeded by $\sim 0.1 \mu\text{J}$ signal: (a) $\lambda_s = 570$ nm, (b) $\lambda_s = 490$ nm.

with $E_p = 70 \mu\text{J}$. Note that the unbalance keeps favoring the red-shifted region, even when the entire number of cascaded blue-shifted side-bands is accounted for.

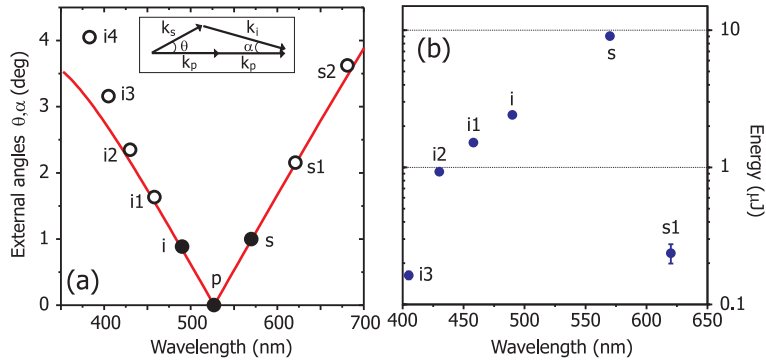


Fig. 4. (a) Phase matching curve for FWOPA pumped by 527 nm pulse (red curve) and measured angles of the parametric waves (open circles). The inset depicts interaction geometry. (b) energy distribution among the parametric waves at $E_p = 70 \mu\text{J}$.

We interpret this asymmetry as the non trivial impact of the absorption on a multi-step parametric process (water absorption increases from the blue toward the near IR, the absorption coefficient being $\alpha = 0.0044 \text{ m}^{-1}$ at 417 nm, and $\alpha = 0.281 \text{ m}^{-1}$ at 625 nm [21]): in the absence of cascading, one should expect absorption to reduce the overall gain of the primary parametric process (amplification of the seed signal accompanied by the generation of the idler wave) without producing any appreciable unbalance. In fact, the propagation length is here too short for direct loss on generated photons to play a role; in the presence cascading, however, absorption unevenly modifies the gain of each particular cascading process. Specifically, large absorption at the first cascading red-shifted sideband ($\lambda_{s1} = 621$ nm) should prevent effective cascading to occur in spite of optimum phase matching, leaving the $\lambda_{s1} = 621$ nm secondary band unexcited and thus the $\lambda_s = 570$ nm primary (signal) band undepleted. In contrast, water transparency in the blue greatly supports blue-shifted cascading, leading to strong depletion of the primary (idler) $\lambda_i = 490$ nm band and excitation of a large number of blue-shifted secondary bands at $\lambda_{i1} = 458$ nm, $\lambda_{i2} = 430$ nm, $\lambda_{i3} = 405$ nm and $\lambda_{i4} = 383$ nm.

In order to explain the measured energy unbalance, we note that cascading not only involves

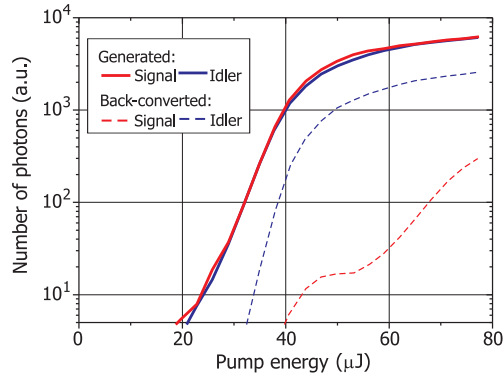


Fig. 5. Calculated photon yield in signal (red) and idler (blue) waves versus pump energy: generated photons N_s^{total} and N_i^{total} (solid curves) and back-converted N_s^{back} and N_i^{back} photons (dashed curves).

the transfer of some amount of photons from primary (signal and idler) to cascaded side bands, but also the transfer (back-conversion) of some amount of photons from primary back to $\lambda_p = 527$ nm pump wave. The results in terms of calculated photon numbers using the experimental data of Fig. 3(a) with account for energy in the cascaded components [an example is shown in Fig. 4(b)] are illustrated in Fig. 5, plotting the total numbers of generated photons N in signal and idler waves. These are calculated in accordance with multi-step FWM processes and yield simple recurrent equations for generated signal $N_s^{\text{total}} = N_s + 2N_{s1} + 3N_{s2}$ and idler $N_i^{\text{total}} = N_i + 2N_{i1} + 3N_{i2} + 4N_{i3} + 5N_{i4}$ photons. The numbers of back-converted photons to the pump are then calculated as $N_s^{\text{back}} = N_{s1} + 2N_{s2}$ and $N_i^{\text{back}} = N_{i1} + 2N_{i2} + 3N_{i3} + 4N_{i4}$. In the calculations we have omitted photon numbers N_{s2} and N_{i4} since they were negligibly small. The fact that calculated number of generated photons in signal and idler waves virtually coincide over a fairly broad range of pump energies, confirms the validity of Manley-Rowe relation on equal number of generated signal and idler photons, if it is suitably extended to the full set of cascading bands. Since the gain for particular cascading process varies with frequency due to absorption, the apparent unbalance in Fig. 3 is due to the difference in the back-converted photon numbers from the blue and red-shifted bands, depicted by the dashed lines in Fig. 5.

3. Conclusion

In conclusion, we have demonstrated an operating condition for highly efficient four-wave parametric amplification in a bulk isotropic medium with Kerr nonlinearity (water) in the visible spectral range. With overall figure of 25% energy conversion from pump to parametric waves, FWOPA is simple and inexpensive frequency converter with high operational characteristics. Cylindrical focusing allows non-collinear phase-matched interaction, which quenches the transverse break up of the pump beam and permits the achievement of 1-dimensional spatial soliton propagation regime. Differently from the filament-mediated four-wave parametric amplification, the spatial soliton regime is not limited in the transverse dimension (along the long axis of an ellipse), so that the setup can be easily scaled in size and energy. And finally, our finding on quenching spontaneous break-up and filamentation of the intense laser beam by launching a weak seed signal opens a new route towards a controllable beam break-up into multiple filaments.

Acknowledgments

P. P. and H. V. acknowledge the support from Sixth EU Framework Programme Contract No. MEST-CF-2004-008048 (ATLAS), P.D.T. acknowledges the support from Marie Curie Chair project STELLA (<http://www.vino-stella.eu>), Contract No. MEXC-CT-2005-025710.

Permanent addresses: * INFN and Department of Physics, University of Insubria, Via Valleggio 11, IT-22100 Como, Italy and ** University of Tartu, Institute of Physics, Riia 142, EE-51014 Tartu, Estonia.